NASA Contractor Report 189710
ICASE Report No. 92-45

ICASE

FULLY NONLINEAR DEVELOPMENT OF THE MOST UNSTABLE GÖRTLER VORTEX IN A THREE DIMENSIONAL BOUNDARY LAYER

S. R. Otto
Andrew P. Bassom

Contract Nos. NAS1-18605 and NAS1-19480
September 1992

Institute for Computer Applications in Science and Engineering
NASA Langley Research Center
Hampton, Virginia 23665-5225

Operated by the Universities Space Research Association

National Aeronautics and
Space Administration

Langley Research Center
Hampton, Virginia 23665-5225

FULLY NONLINEAR DEVELOPMENT OF THE MOST UNSTABLE GÖRTLER VORTEX IN A THREE DIMENSIONAL BOUNDARY LAYER

S. R. Otto*
ICASE, Mailstop 132c
NASA Langley Research Center
Hampton, VA 23665-5225, USA

Andrew P. Bassom
Department of Mathematics
University of Exeter, North Park Road
Exeter, Devon, EX4 4QE, UK

ABSTRACT

In this paper we investigate the nonlinear development of the most unstable Görtler mode within a general three-dimensional boundary layer upon a suitably concave surface. The structure of this mode was first identified by Denier, Hall & Seddougui (1991) who demonstrated that the growth rate of this instability is $O(G^{\frac{3}{5}})$ where G is the Görtler number (taken to be large here), which is effectively a measure of the curvature of the surface. Previous researches have described the fate of the most unstable mode within a two-dimensional boundary layer. Denier & Hall (1992) discussed the fully nonlinear development of the vortex in this case and showed that the nonlinearity causes a breakdown of the flow structure.

The effect of crossflow and unsteadiness upon an infinitesimal unstable mode was elucidated by Bassom & Hall (1991). They demonstrated that crossflow tends to stabilise the most unstable Görtler mode, and for certain crossflow/frequency combinations the Görtler mode may be made neutrally stable. These vortex configurations naturally lend themselves to a weakly nonlinear stability analysis; work which is described in a previous article by the present authors. Here we extend the ideas of Denier and Hall (1992) to the three-dimensional boundary layer problem. It is found that the numerical solution of the fully nonlinear equations is best conducted using a method which is essentially an adaption of that utilised by Denier and Hall (1992). The influence of crossflow and unsteadiness upon the breakdown of the flow is described.

* Research was supported by the National Aeronautics and Space Administration under NASA contracts Nos. NAS1-18605 and NAS1-19480 while the author was in residence at the Institute for Computer Applications in Science and Engineering (ICASE), NASA Langley Research Center, Hampton, VA 23665

§1 Introduction

The aim of this article is to further our understanding of the effects of unsteadiness and crossflow upon the fully nonlinear development of unstable Görtler modes. The initial derivation of the governing equations for these modes was given by Görtler (1940) whose results were modified by Hammerlin (1956). These early works ignored nonparallel effects present due to boundary layer growth and Smith (1955) added terms in an attempt to rectify this deficiency. Until recent years it was unclear as to the importance of the nonparallel terms; this question was resolved by the results of Hall (1982 a,b, 1983). In this series of papers Hall showed, using a combination of asymptotic and numerical techniques, that for order one wavenumber vortices there is no unique neutral linear stability curve. More precisely, the stability characteristics of such wavenumber modes are entirely dependent upon the initial form and location of the disturbance. However for small wavelength vortices a unique neutral curve does exist and on this curve the vortex wavenumber k is $O(G^{\frac{1}{4}})$ where G is the (assumed large) Görtler number. For further reading concerning the development of the stability theory for Görtler vortices the reader is referred to Hall (1990).

The most unstable Görtler mode (i.e. that infinitesimally-sized vortex which has the largest growth rate) was obtained by Denier, Hall & Seddougui (1991) and Timoshin (1990). By considering the stability properties of the essentially viscous modes of wavenumber $O(G^{\frac{1}{4}})$ together with those of the inviscid modes of $O(1)$ wavelengths it was possible to identify an intermediate wavenumber regime in which the vortex growth rate is largest. These unstable modes are confined to a region of depth of $O(G^{-\frac{1}{5}})$ and possess growth rates of size $O(G^{\frac{3}{5}})$. The stability properties of $O(G^{\frac{1}{5}})$ wavenumber vortices are deduced by solving a sixth-order ordinary differential system with appropriate boundary conditions and the solution of this system reveals that the unique most unstable mode has wavenumber $k = 0.476G^{\frac{1}{5}}$ and growth rate $0.312G^{\frac{3}{5}}$.

To date there has been relatively little attention paid to the nonlinear stability properties of Görtler vortices. Perhaps the first work was performed by Aihara (1976) who attempted to describe the nonlinear evolution of Görtler vortices using parallel arguments. Later calculations by Hall (1988) remedied these defects and showed that as $O(1)$ wavenumber modes evolve downstream so the energy of the flow concentrates itself in the fundamental and mean flow correction. This suggests far downstream the flow can be adequately described by a mean field/first harmonic structure and such a configuration was elucidated for short wavelength modes using both weakly nonlinear and fully nonlinear approaches by Hall (1982 b) and Hall & Lakin (1988) respectively.

A fuller description of the nonlinear stability of Görtler modes may be found in Denier & Hall (1992). In that paper the authors argued that in a number of practical systems, especially where significant curvature occurs such as the case of flow over

turbine blades, one would expect the small localized surface imperfections may well trigger the most unstable linear Görtler mode. (This conclusion relies on the result of the linear receptivity theory given by Denier, Hall & Seddougui (1991).) This motivated a careful study of nonlinear evolution of the most unstable mode which was tackled in the following way. Denier & Hall (1992) took an arbitrary form of initial disturbance at a typical streamwise location, say $x = 1$. By integrating the *linear* form of the vortex equations over a long distance, up to $x = 101$, a flow profile was obtained which is dominated by the most unstable mode described by Denier *et al* (1991). From $x = 101$ onwards the full nonlinear equations replaced the linear ones and the most unstable vortex mode was marched further. Typically 8 or 16 harmonics of the fundamental were retained during this calculation. It was found that at a critical point the flow contains a region of reverse flow and the analysis is then no longer valid. Denier & Hall (1992) interpreted this breakdown as being responsible for the vortices moving away from the wall and into the core of the boundary layer.

The effect of crossflow and unsteadiness on the most unstable Görtler mode was discussed by Bassom & Hall (1991). The primary result arising from this work was the demonstration that a relatively small crossflow could completely stabilise the most unstable mode. Additionally, by allowing for vortex unsteadiness, it was shown that suitable combinations of crossflow, vortex frequency and wavenumber could lead to neutrally stable configurations. A weakly nonlinear stability analysis pertaining to such configurations was conducted by Bassom & Otto (1992) who derived classical 'Stuart–Watson' (1960) type evolution equations for near–neutral modes. They concluded that the weak–nonlinearity has a stabilising effect and derived equations for the supercritical equilibrium amplitudes.

The results of Denier & Hall (1992) and Bassom & Hall (1991) provide the motivation for the current study. Within a two–dimensional boundary layer the effect of nonlinearity on the most unstable mode tends to lead to a finite–distance breakdown whereas crossflow appears to stabilise the flow. With these two mechanisms tending to have opposite effects it is clear that in many practical situations, where three–dimensionality is undoubtedly important, it is of great interest to determine which of these two conflicting behaviours dominate. We attempt to answer this question by considering the full nonlinear vortex equations and employ numerical techniques which are similar to those used in Denier & Hall (1992) but modified in certain ways (detailed later). These improvements significantly speed up the computations and allow us to obtain a greater range of results than those found by Denier & Hall (1992).

The structure of the remainder of this article is as follows: in section 2 the fully nonlinear equations are derived and a brief description of the numerical procedures

used are outlined in section 3. Details of the results are presented in section 4 and in section 5 some brief conclusions are drawn.

§2 Formulation

As in Hall (1985) we consider a boundary layer flowing over the cylinder $\tilde{y} = 0$, $-\infty < \tilde{z} < \infty$ where the $\tilde{z}$–axis is a generator of the cylinder, $\tilde{y}$ measures the distance normal to the surface and $\tilde{x}$ denotes the distance along the surface. The Reynolds number R_e and Görtler number G are defined by

$$R_e = \frac{U_0 L}{\nu}, \qquad G = 2R_e^{\frac{1}{2}}\delta,$$

where U_0 is a typical flow velocity in the $\tilde{x}$–direction, L is a characteristic streamwise lengthscale and ν is the kinematic viscosity of the fluid. Furthermore the curvature of the cylinder is supposed to be $\frac{1}{b}\chi_0\left(\frac{\tilde{x}}{L}\right)$ and with these definitions $\delta \equiv L/b$, where b is a typical radius of curvature of the cylinder (Görtler vortices are typically observed in flows over concave surfaces which corresponds to the choice $\chi_0 > 0$). The Reynolds number is supposed to be large whilst δ is sufficiently small so that as $\delta \to 0$ the parameter G is fixed and is of order one. The basic three–dimensional boundary layer is taken to be of the form

$$\mathbf{u} = U_0\left(\bar{u}(X,Y), R_e^{-\frac{1}{2}}\bar{v}(X,Y), R_e^{-\frac{1}{2}}\lambda^*\bar{w}(X,Y)\right)\left(1 + O\left(R_e^{-\frac{1}{2}}\right)\right)$$

where $X = \tilde{x}/L$ and $Y = \tilde{y}R_e^{\frac{1}{2}}/L$ and the crossflow parameter λ^* is of order one.

It is convenient to define the scaled spanwise coordinate $Z = \tilde{z}R_e^{\frac{1}{2}}/L$ and let T be the temporal variable scaled on L/U_0. The basic velocity profile is perturbed by the quantity

$$\left(U(T,X,Y,Z), R_e^{-\frac{1}{2}}V(T,X,Y,Z), R_e^{-\frac{1}{2}}W(T,X,Y,Z)\right),$$

and the pressure field by $R_e^{-\frac{1}{2}}P(T,X,Y,Z)$. Substituting this flow form into the continuity and Navier–Stokes equations yields the system

$$U_X + V_Y + W_Z = 0, \tag{2.1a}$$

$$\begin{aligned} -U_T + U_{YY} + U_{ZZ} - \bar{u}_Y V - \bar{u}U_X - \bar{u}_X U - \bar{v}U_Y - \lambda^*\bar{w}U_z \\ = UU_X + VU_Y + WU_Z, \end{aligned} \tag{2.1b}$$

$$\begin{aligned} -V_T + V_{YY} + V_{ZZ} - G\chi\bar{u}U - P_Y - \bar{u}V_X - \bar{v}_X U - \bar{v}V_Y - \bar{v}_Y V - \lambda^*\bar{w}V_z \\ = UV_X + VV_Y + WV_Z + \frac{G}{2}\chi U^2, \end{aligned} \tag{2.1c}$$

$$-W_T + W_{YY} + W_{ZZ} - P_Z - \overline{u}W_X - \lambda^*\overline{w}_X U - \overline{v}W_Y - \lambda^* V\overline{w}_Y - \lambda^*\overline{w}W_z = UW_X + VW_Y + WW_Z, \tag{2.1d}$$

where terms of relative order $O(R_c^{-\frac{1}{2}})$ have been neglected. It is worth noting at this point that the linearised system studied by Bassom & Hall (1991) is obtained by setting the right-hand sides of (2.1 b-d) to zero whereas the nonlinear equations examined by Denier & Hall (1992) to determine the development of steady nonlinear vortices in two-dimensional boundary layers can be retrieved by setting λ^* and ∂_T equal to zero.

We now invoke the scalings proposed by Denier *et. al.* (1991) who demonstrated that in high Görtler number flows the most unstable vortices have $O(G^{\frac{1}{5}})$ wavenumbers and are confined to a layer of thickness of $O(G^{-\frac{1}{5}})$ adjacent to the cylinder. These modes have a spatial growth rate of $O(G^{\frac{3}{5}})$ and we use the results of Bassom & Hall (1991) who illustrated that the three-dimensionality of the basic flow significantly affects the two-dimensional stability results once the scaled crossflow parameter λ^* becomes $O(G^{\frac{3}{5}})$. Therefore it is convenient to define the $O(1)$ crossflow parameter $\hat{\lambda}$ by

$$\lambda^* = G^{\frac{3}{5}}\hat{\lambda}. \tag{2.2a}$$

To reflect the fact that the vortices are confined to a region of depth $O(G^{-\frac{1}{5}})$ adjacent to the cylinder we introduce the $O(1)$ boundary layer coordinate y defined by

$$y = G^{\frac{1}{5}}Y, \tag{2.2b}$$

and in this layer the basic flow may be expanded as a Maclaurin series of the form

$$\bar{u} = G^{-\frac{1}{5}}\mu_{11}(X)y + \tfrac{1}{2}G^{-\frac{2}{5}}\mu_{12}(X)y^2 + \tfrac{1}{6}G^{-\frac{3}{5}}\mu_{13}(X)y^3 + \cdots \quad , \tag{2.2c}$$

$$\bar{w} = G^{-\frac{1}{5}}\mu_{21}(X)y + \tfrac{1}{2}G^{-\frac{2}{5}}\mu_{22}(X)y^2 + \tfrac{1}{6}G^{-\frac{3}{5}}\mu_{23}(X)y^3 + \cdots \quad . \tag{2.2d}$$

To determine the form of the vortex disturbance we appeal to the findings of Bassom & Otto (1992) who identified the crucial perturbation size at which the governing equations become fully nonlinear (although these authors made no attempt to solve these fully nonlinear forms). The disturbance forms are then

$$U = G^{-\frac{1}{5}}\left(U_0 + G^{-\frac{1}{5}}U_1 + G^{-\frac{2}{5}}U_2 + \cdots\right), \qquad V = G^{\frac{1}{5}}\left(V_0 + G^{-\frac{1}{5}}V_1 + G^{-\frac{2}{5}}V_2 + \cdots\right). \tag{2.3a, b}$$

$$W = G^{\frac{2}{5}}\left(W_0 + G^{-\frac{1}{5}}W_1 + G^{-\frac{2}{5}}W_2 + \cdots\right), \qquad P = G^{\frac{2}{5}}\left(P_0 + G^{-\frac{1}{5}}P_1 + G^{-\frac{2}{5}}P_2 + \cdots\right), \tag{2.3c, d}$$

where U_0, V_0, W_0, P_0, U_1, ... etc. are all functions of X, y, the temporal and the spanwise variable. It is now convenient to implement the result of Bassom & Hall (1991)

that the leading order behaviour in the downstream coordinate is purely oscillatory and we do this by introducing the coordinate and temporal variations given by

$$X = G^{-\frac{3}{5}}x, \qquad Z = \beta x + G^{-\frac{1}{5}}z, \qquad T = G^{-\frac{2}{5}}t, \tag{2.4a}$$

where $\beta = \hat{\lambda}\mu_{21}/\mu_{11}$. This then implies that the streamwise and spanwise derivatives become

$$\frac{\partial}{\partial X} \to G^{\frac{3}{5}}\frac{\partial}{\partial x} - \beta G^{\frac{4}{5}}\frac{\partial}{\partial z}, \qquad \frac{\partial}{\partial Z} \to G^{\frac{1}{5}}\frac{\partial}{\partial z}. \tag{2.4b}$$

The desired governing equations are obtained by substituting (2.2)-(2.4) into equations (2.1). Leading order terms in the momentum equations yield that $W_0 = \beta U_0$. Next order terms in equation (2.1 b) give the first relationship

$$\left(\frac{\partial^2}{\partial y^2} + \frac{\partial^2}{\partial z^2} - \frac{y^2\alpha}{2}\frac{\partial}{\partial z} - \frac{\partial}{\partial T} - \mu_{11}y\frac{\partial}{\partial x}\right)U_0 - \mu_{11}V_0 = \mathrm{RHS}_1, \tag{2.5a}$$

where the precise form of RHS_1 is given presently and $\alpha = \hat{\lambda}\mu_{22} - \beta\mu_{21}$. A second equation is derived by following a procedure similar to that described by Bassom & Hall (1991). By considering the second order terms in the y and z momentum equations (2.3), eliminating the pressure by cross-differentiation and applying the continuity equation it is a routine but lengthy task to obtain

$$\left(\frac{\partial^2}{\partial y^2} + \frac{\partial^2}{\partial z^2} - \frac{y^2\alpha}{2}\frac{\partial}{\partial z} - \frac{\partial}{\partial T} - \mu_{11}y\frac{\partial}{\partial x}\right)\left(\frac{\partial^2}{\partial y^2} + \frac{\partial^2}{\partial z^2}\right)V_0 + \alpha\frac{\partial V_0}{\partial z} - \chi_0\mu_{11}y\frac{\partial^2 U_0}{\partial z^2} = \mathrm{RHS}_2 \tag{2.5b}$$

where again we shall specify RHS_2 shortly. The forms of RHS_2 includes reference to the combination $W_1 - \beta U_1$ which therefore needs to be expressed in terms of quantities with subscript zero. This is best accomplished by integrating the continuity equation to give

$$W_1 - \beta U_1 = \phi_0(x, y) - \int\left[\frac{\partial U_0}{\partial x} + \frac{\partial V_0}{\partial y}\right]dz. \tag{2.5c}$$

The aim of this article is to consider the nonlinear evolution of modes which are periodic in the spanwise direction, with fundamental wavenumber $(\chi_0\mu_{11}^2)^{\frac{1}{5}}k$ say, and periodic in time. Now it is advantageous to introduce scalings first proposed by Bassom & Hall (1991). It is found that if we transform according to

$$\partial_y \to (\chi_0\mu_{11}^2)^{\frac{1}{5}}k\partial_y, \qquad \partial_z \to (\chi_0\mu_{11}^2)^{\frac{1}{5}}k\partial_z, \qquad \partial_x \to \chi_0^{\frac{3}{5}}\mu_{11}^{\frac{1}{5}}\partial_x, \tag{2.6a-c}$$

$$U_0 = \chi_0^{-\frac{1}{5}}\mu_{11}^{\frac{3}{5}}U, \qquad V_0 = \chi_0^{\frac{1}{5}}\mu_{11}^{\frac{2}{5}}V, \qquad \partial_T \to \chi_0^{\frac{2}{5}}\mu_{11}^{\frac{4}{5}}\partial_T, \tag{2.6d-f}$$

$$\phi_0 = \chi_0^{\frac{2}{5}}\mu_{11}^{\frac{4}{5}}\bar{\phi}, \qquad \lambda = \frac{\hat{\lambda}(\mu_{11}\mu_{22} - \mu_{21}\mu_{12})}{2\mu_{11}^{\frac{1}{5}}\chi_0^{\frac{3}{5}}}, \tag{2.6g-h}$$

then the transformed equations (2.5 a,b) are independent of the particular boundary layer under consideration. Therefore the ensuing results are potentially relevant to a wide class of basic configurations. In this nondimensionalised coordinate system we restrict ourselves to flow quantities the fundamental mode having spanwise and temporal variation given by $\exp\left[i\left(z+\bar{\Omega}t\right)\right]$, so that $\bar{\Omega}$ represents the nondimensional frequency of the fundamental vortex component.

Upon making the transformations (2.6) the leading order vortex equations (2.5 a,b) become

$$L\left(\frac{\partial^2}{\partial y^2}+\frac{\partial^2}{\partial z^2}\right)V+\frac{2\hat{\lambda}}{k^3}\frac{\partial V}{\partial z}-\frac{y}{k^3}\frac{\partial^2 U}{\partial z^2}=\frac{1}{k^2}\frac{\partial^2 S^{(1)}}{\partial z^2}-\frac{1}{k^2}\frac{\partial^2 S^{(2)}}{\partial z\partial y}-\frac{1}{k^3}\frac{\partial^2 S^{(3)}}{\partial x\partial y}, \tag{2.7a}$$

$$L\left(U\right)-\frac{V}{k^2}=\frac{1}{k^2}S^{(3)}, \tag{2.7b}$$

where the operator L is defined according to

$$L\left[\psi\right]=\frac{\partial^2\psi}{\partial y^2}+\frac{\partial^2\psi}{\partial z^2}-\frac{\lambda y^2}{k^3}\frac{\partial\psi}{\partial z}-\frac{1}{k^2}\frac{\partial\psi}{\partial T}-\frac{y}{k^3}\frac{\partial\psi}{\partial x}, \tag{2.7c}$$

and

$$S^{(1)}=U\frac{\partial V}{\partial x}+kV\frac{\partial V}{\partial y}+k\frac{\partial V}{\partial z}\left[\bar{\phi}-\frac{1}{k}\int_z\left[\frac{\partial U}{\partial x}+k\frac{\partial V}{\partial y}\right]dz\right]+U^2, \tag{2.7d}$$

$$\begin{aligned}S^{(2)}=&U\frac{\partial}{\partial x}\left[\bar{\phi}-\frac{1}{k}\int_z\left[\frac{\partial U}{\partial x}+k\frac{\partial V}{\partial y}\right]dz\right]\\&+Vk\frac{\partial}{\partial y}\left[\bar{\phi}-\frac{1}{k}\int_z\left[\frac{\partial U}{\partial x}+k\frac{\partial V}{\partial y}\right]dz\right]\\&-\left[\bar{\phi}-\frac{1}{k}\int_z\left[\frac{\partial U}{\partial x}+k\frac{\partial V}{\partial y}\right]dz\right]\left(\frac{\partial U}{\partial x}+k\frac{\partial V}{\partial y}\right),\end{aligned} \tag{2.7e}$$

$$S^{(3)}=U\frac{\partial U}{\partial x}+kV\frac{\partial U}{\partial y}+k\frac{\partial U}{\partial z}\left[\bar{\phi}-\frac{1}{k}\int_z\left[\frac{\partial U}{\partial x}+k\frac{\partial V}{\partial y}\right]dz\right]. \tag{2.7f}$$

To complete the governing equations it is necessary to determine $\bar{\phi}$. This is achieved by noticing that $W_1-\beta U_1$ satisfies

$$L\left(W_1-\beta U_1\right)=\alpha y V_0+\frac{\partial P_0}{\partial z}+S^{(2)}.$$

Identifying the component of this equation independent of z yields

$$2\pi\left[\frac{\partial^2}{\partial y^2}-\frac{y}{k^3}\frac{\partial}{\partial x}\right]\bar{\phi}=\frac{1}{k^2}\int_0^{2\pi}\left\{yV\frac{\lambda}{k}+S^{(2)}\right\}dz. \tag{2.7g}$$

To close the system requires specification of appropriate boundary conditions. Clearly we require the velocity components U, V to vanish on $y = 0$ (and by continuity so must $\partial V/\partial y$). Additionally the mean flow terms $\phi = 0$ on $y = 0$ and in order that the disturbance be confined to the boundary layer we demand that the streamwise velocity U tends to some function of x as $y \to \infty$.

We notice that equations (2.7) are the appropriate generalisations of those solved by Denier and Hall for the most unstable nonlinear vortex within a two dimensional boundary layer (their equations are recovered by setting $\hat{\lambda} = \phi = 0$ and setting ∂_T=0). This allowed us to compare numerical results against their previously published ones as a check of our numerical methods.

§3 Numerical Methods

The methods employed to solve system (2.7) are similar in essence to those used in Denier & Hall (1992). However it was found necessary to introduce a number of amendments to their code in order to speed up the computations which in turn had the benefit of allowing an increased number of results to be obtained.

Denier & Hall (1992) solved the two-dimensional counterparts of equations (2.7) as follows. They decomposed each of the flow velocities U, V, W into their Fourier components and rewrote the governing equations in terms of these components. By utilising a scheme based upon that implemented by Hall (1988) they obtained finite-difference equations for the mean flow and harmonic terms. These equations contain only one streamwise derivative and a straightforward method, based upon solving one tridiagonal and one pentadiagonal system, may be used to march the solution from one streamwise station to the next. For more details of the practicalities of the scheme the reader is referred to Denier & Hall (1992).

One marked difference between our present work and that of Denier & Hall (1992) is that we chose to calculate the nonlinear terms in physical space rather than transform space, as this is a computationally 'cheaper' policy and so allowed us to retain more modes in our calculations. This necessitates transforming from Fourier space to physical space, effecting the calculations and extracting the Fourier coefficients. It was decided to employ Fast Fourier Transforms to do this which has the benefit of reducing the cost of the transformations from $O(N^2)$, (the cost of reducing N modes and using the Fourier transform directly) to $O(5N \log N - 6N)$. The code used was based on the original Cooley and Tukey (1965) algorithm and was thus limited to N being an integral power of 2.

Two other changes were made to the code used by Denier & Hall (1992). As was described in the introduction, these authors were concerned with the development of the most unstable Görtler mode within a two-dimensional boundary layer. To

achieve this most unstable mode Denier & Hall (1992) took an arbitrary disturbance and then marched the linear stability equations for a long distance downstream before changing to the nonlinear system. This of course had the effect of ensuring that the most unstable component of the original disturbance was then dominant over all the other components so that when the full nonlinear equations were invoked the input vortex flow was dominated by the most unstable mode. A drawback of this method is that the lead–in time in which the linear mode develops proves to be a significant proportion of the total computation time. To alleviate this difficulty we used the program described by Bassom & Otto (1992) to compute the unstable eigenfunction directly. This had the effect of making the lead–in time to the nonlinear equations redundant and thus we could start our computations of the full nonlinear system almost immediately. Substantial reduction in the computational time was also achieved by using a stretched grid in the y–direction (normal to the cylinder surface) as opposed to a uniform one, and the scheme eventually chosen for this process was taken from Macaraeg, Streett & Hussaini (1988). A grid is required which encompasses the region between $y_p = 0$ and $y_p = y_{max}$, where the subscript p denotes the physical coordinate and y_{max} denotes some outer bound at which the asymptotic forms of the solution of the system (2.7) are supposed to have been attained. A notional computational grid $0 \leq y_c \leq 1$ is introduced which is related to y_p via

$$y_p = \frac{y_{max}\,(c_2 - 1)^{c_1}\, y_c}{(c_2 - y_c^2)^{c_1}},$$

with the value $(c_2 - 1)$ taking values between 0.2 and 1. The quantity $(c_2 - 1)$ represents the degree of stretching between the large and small steps whilst c_1 controls the rate of stretching, $1 \leq c_1 \leq 6$. For most of the calculations reported here we used $c_1 = 2.4$ and $c_2 = 2$ which allows 100 grid points to be distributed between $y_p = 0$ and $y_p = 50$. The resulting distribution of points and the corresponding step lengths are illustrated in figure 1. Notice that as $y \to y_{max}$ the step lengths become greater than unity which in a finite difference scheme may induce errors. In the present case gradients of the dependent functions in this regime are minuscule and so this possible difficulty did not arise. This particular non–uniform stretching of the grid points allowed a twenty–fold reduction in the number of grid points over the regular grid used in Bassom & Hall (1991) and a four–fold improvement over the piecewise constant step length grid used in Bassom & Otto (1992).

As previously mentioned the solution strategy used here is essentially that described in Hall (1988). Suppose that the solution $(U_0, V_0, U_{0x}, \phi_0)$ is known at some specified station, x, and suppose further that a guess is made for the solution at $x + \epsilon$, $\left(U_1^{(0)}, V_1^{(0)}, \phi_1^{(0)}\right)$. The nonlinear terms on the right–hand sides of equations (2.7 a,b)

were calculated using these guesses and the system solved to provide updated values $\left(U_1^{(1)}, V_1^{(1)}, \phi_1^{(1)}\right)$. These updated variations were then put into the nonlinear terms and the process repeated. When the difference between successive iterates was than some norm convergence was deemed to have occurred and this process marched onto the next step. For a computational grid composed of M points and a calculation with N modes retained then the convergence norm used was

$$\sum_{k=-N/2}^{k=N/2-1} \sum_{j=1}^{j=M} \left[|U_{j,k}^{(n+1)} - U_{j,k}^{(n)}| + |V_{j,k}^{(n+1)} - V_{j,k}^{(n)}| \right] < 10^{-6} N.$$

where $U_{j,k}^{(n)}$ denotes the n^{th} iterate of the k^{th} Fourier component of the flow quantity U evaluated at the j^{th} y–position.

The equations (2.7 a,b) may be discretised for any particular mode into the forms

$$a_m v_{m+2} + b_m v_{m+1} + c_m v_m + d_m v_{m-1} + e_m v_{m-2} + f_m u_m = V_m, \qquad (m = 3, \cdots M-1) \tag{3.1a}$$

and

$$g_m u_{m+1} + h_m u_m + i_m u_{m-1} + j_m v_m = U_m. \qquad (m = 2, \cdots M-1) \tag{3.1b}$$

This system was solved using a technique outlined in Appendix B of Bassom & Otto (1992). This solves the problem (3.1) in one sweep rather than treating the pair (3.1 a,b) as distinct pentadiagonal and tridiagonal problems. In essence, the equations are solved by performing an outward forward elimination followed by a back substitution.

Earlier we alluded to the fact that significant computational saving was obtained by utilising Fast Fourier Transforms in preference to decomposing the flow quantities into their respective components. Standard procedures were implemented so that to change between physical and transform spaces we write

$$\psi_j = \sum_{k=-\frac{N}{2}}^{k=\frac{N}{2}} \tilde{\psi} e^{ikz_j}, \qquad j \in [1, N],$$

$$\tilde{\psi}_k = \frac{1}{N} \sum_{j=1}^{j=N} \psi e^{-ikz_j}, \qquad k \in [-\frac{N}{2}, \frac{N}{2} - 1],$$

where $z_j = 2\pi(j-1)/N$ for $j \in [1, N]$ and where quantities with tildes are in the transform space and those without in the physical space. Denier & Hall (1992) were able to restrict themselves to using a cosine basis due to the nature of Görtler vortices

with two–dimensional boundary layers but the addition of temporal periodicity and crossflow prevented us from doing this.

For the majority of the calculations presented below the number of modes retained was 16 and a fairly large step used in the streamwise direction, typically $\epsilon = 0.01$. Denier & Hall (1992) found in their calculations that these parameter choices gave results to within graphical accuracy. Further testing, using 100 points in the normal direction and with $y_{max} = 50$ has confirmed that similar choices are satisfactory for the three–dimensional computations performed here.

§4 Results

We have detailed the numerical method by which we investigated the solution properties of system (2.7) although as yet we have left the definition of the amplitude of the initial vortex unspecified. As described, we initiated our computations with a multiple of the eigenfunctions of the linearised versions of system (2.7). For a specified vortex wavenumber k, frequency $\bar{\Omega}$ and crossflow $\hat{\lambda}$ the method outlined by Bassom & Otto (1992) was used to compute the corresponding linearised growth rates β_r and the respective eigenfunctions normalised so that the energy defined by

$$\int_{y=0}^{y=\infty} (U^2 + V^2) dy$$

is equal to Δ^2. We refer to Δ as the amplitude of the initial condition.

Our first calculations were performed primarily as a verification of our code against the established results of Denier & Hall (1992). Thence we considered the case of a purely two-dimensional boundary layer and steady vortices ($\hat{\lambda} = \bar{\Omega} = 0$). Denier & Hall (1992) found that as the vortex evolves nonlinearly downstream then at some point their computations broke down in a singularity. Careful investigation revealed that at this location the skin friction was of the flow vanishes and then any solution scheme which relies upon a marching technique becomes invalidated. The vanishing of the skin friction was interpreted as being indicative of the vortices breaking away from the wall and moving into the core of the boundary layer. Our results for various initial amplitudes Δ are indicated on figure 2 where we show the location of the breakdown point x_b as a function of Δ for the most unstable Görtler mode with vortex wavenumber $k = 0.476$ (the disturbance was introduced at $x = 1$ so the distance travelled by the perturbation before breakdown is $x_b - 1$). Not surprisingly, the breakdown location x_b is a monotone decreasing function of the amplitude Δ and as $\Delta \to 0$ so $x_b \to \infty$ and the linear problem is retrieved. For all the other calculations reported upon here a similar trend is observed so that in all cases we chose $\Delta = 0.2$; this selection was made purely for illustrative purposes and has no special significance whatsoever.

In figure 3 we demonstrate another feature of the two–dimensional results. Figure 3a indicates the dependence of the linear vortex growth rate β_r as a function of the vortex wavenumber k for the first two modes. As is now well documented by Denier *et al.* (1991), Denier & Hall (1992) the most unstable mode has growth rate $\beta_r = 0.312$ at $k = 0.476$ and $\beta_r \to 0$ as $k \to 0$ or $k \to \infty$. We note however, that for a significant range of scaled wavenumbers, roughly $0.3 \leq k \leq 0.8$, the vortex growth rate is not much reduced from the maximum in as much as it is at least 90% of the maximum. This will have important consequences for later results. Figure 3b illustrates breakdown point x_b as a function of k for the first two modes. As is to be expected for fixed initial amplitude Δ and fixed wavenumber the first mode always breaks away from the wall before the second one and this trend continues for higher modes. However, it is also observed that for the primary mode, x_b is a monotone decreasing function of k. Therefore for any fixed initial amplitude it is not the most unstable mode which breaks up first. Indeed we previously remarked that for a whole range of wavenumbers surrounding the most unstable value linear growth rates are not too different from the largest growth rate. This has potentially important consequences for a number of practical flows as it demonstrates that the breakdown properties of the flow are crucially dependent on the nature of the physical characteristics of the flow and are sensitive to the nature of the evolution of the flow. More precisely, suppose that the vortex motion starts with extremely small amplitude. Then one would expect there to be a large distance over which the motion develops essentially in a linear manner. During this time the most unstable linear mode would overwhelm modes of other wavelengths and once the vortices had grown sufficiently so that nonlinearity is important the flow behaviour would be dominated by that of the most unstable mode. On the other hand if the initial vortex amplitude is not tiny, nonlinear effect are likely to be important a relatively short distance downstream by which stage it is unlikely that the most unstable mode dominates the others. In this case the behaviour of the most unstable vortex is not likely to dictate the properties of the breakdown of the flow.

We turn now to consider cases with non–zero crossflows. As noted by Bassom & Hall (1991) we may restrict our attention to cases in which the crossflow parameter $\hat{\lambda} > 0$ since by suitably transforming the system (2.7) we can relate flows with $\hat{\lambda} < 0$ to appropriate counterparts with $\hat{\lambda} > 0$. In figure 4 we recall the results of increasing crossflow on the linear, stationary vortex mode. As discussed in detail by Bassom & Hall (1991) the effect of crossflow on linear vortex structures of wavelength $O(G^{-\frac{1}{5}})$ is primarily a stabilising one. Indeed figure 4 illustrates that when $\hat{\lambda} \geq 0.410$ the vortex mode is stabilised for all wavenumbers in the $O(G^{\frac{1}{5}})$ regime.

Figures 5 a& b show the variations of the maximum growth rate $(\beta_r)_{max}$ and the corresponding vortex wavenumber k_{max} for increasing crossflow parameter $\hat{\lambda}$. As already noted, increasing $\hat{\lambda}$ lowers $(\beta_r)_{max}$ and it is the mode with wavenumber $k \sim 0.407$ which is the last to be stabilised. Further k_{max} is not a monotone function of $\hat{\lambda}$ as might have been anticipated. Figure 5b, as well as showing $(\beta_r)_{max}$, indicates the growth rate of the mode with wavenumber $k = 0.476$ (the value of k_{max} for the case of zero crossflow). It can be seen that the difference in growth rates of the most unstable mode and that with $k = 0.476$ is very small over the whole range of $\hat{\lambda}$ considered. This reinforces the earlier comment that there is a significant wavenumber regime over which the linear growth rate of the vortex mode is almost constant.

For each crossflow $\hat{\lambda}$ we integrated the appropriate most unstable linear eigenmode with initial amplitude $\Delta = 0.2$ until breakdown occurred, and then repeated the experiment with vortex wavenumber $k = 0.476$. The results are summarised in figure 5c. It is seen that as well as exercising a stabilising influence on the linear mode, increasing the crossflow tends to have a similar effect on the nonlinear modes. Clearly the greater $\hat{\lambda}$, the greater the delay downstream before the initially most unstable mode breaks away from the wall. Additionally, for the same initial amplitude Δ and crossflow $\hat{\lambda}$ the mode with $k = 0.476$ breaks up before the linearly most unstable mode. Further investigations have suggested that for all choices of $\hat{\lambda}$ and vortex frequency $\bar{\Omega}$ then if two linear modes of different modes $k_1 > k_2$ are such that if initially have the same amplitude then if they are marched downstream then it is the one with the higher wavenumber which breaks down first.

Finally, we discuss in more detail the influence of unsteadiness on our findings. In their study Bassom & Hall (1991) made some comments concerning the properties of time–dependent linearised vortices. For the majority of their work these authors were primarily interested in examining neutrally stable modes although they did compute a few non–neutral ones (see their figure 16). Bassom & Otto (1992) showed that for fixed wavenumber k then as the frequency $\bar{\Omega}$ of the mode increases so the crossflow required to maintain neutral stability grows. In particular it was shown that for a non–dimensional vortex frequency $\bar{\Omega}$ the stability properties of the vortex are sensitive to the sign of $\bar{\Omega}$. In figures 6 a& b we illustrate a facet of this sensitivity. For each frequency $\bar{\Omega}$ and crossflow parameter $\hat{\lambda}$ we show the wavenumber of the most unstable linear mode, k_{max}, together with the growth rate of that mode $(\beta_r)_{max}$. For $\bar{\Omega} < 0$, it it is observed that as $\hat{\lambda}$ increases from zero so k_{max} decreases whereas for $\bar{\Omega} > 0$ this is not the case. Correspondingly, when $\bar{\Omega} < 0$ the growth rate of the most unstable mode is monotone decreasing in $\hat{\lambda}$ whereas when $\bar{\Omega} > 0$ then as $\hat{\lambda}$ increases from zero so there is a crossflow range over which $(\beta_r)_{max}$ increases. This increase is not indefinite however and there is a critical $\hat{\lambda}$, dependent upon $\bar{\Omega}$, after which the growth rate

decreases. We also note that if $\Omega_1 > \Omega_2 > 0$ then $\max_{\hat{\lambda}} \beta_r \left(\bar{\Omega}_1; \hat{\lambda}\right) < \max_{\hat{\lambda}} \beta_r \left(\bar{\Omega}_2; \hat{\lambda}\right)$ so that over all $\bar{\Omega}$ and all $\hat{\lambda} > 0$ the mode with the greatest growth rate is stationary and exists in a two-dimensional boundary layer.

The breakdown characteristics of unsteady flows are described by figure 6c. For each frequency $\bar{\Omega}$ and $\hat{\lambda}$ we marched the linearly most unstable mode of amplitude $\Delta = 0.2$ from $x = 1$. We can observe the somewhat conflicting roles played by crossflow and frequency.

In the main, for a prescribed $\bar{\Omega}$ increasing $\hat{\lambda}$ delays breakdown whereas for fixed $\hat{\lambda}$ and increasing $\bar{\Omega}$ this phenomenon is enhanced. Notice, however, one important feature which runs against this general rule. For positive $\bar{\Omega}$ then a small to moderate crossflow actually tends to promote breakdown although larger crossflows do reverse this effect. An attempt was made to verify this trend by considering larger values of $\bar{\Omega}$ than those illustrated in figure 6. However problems were encountered as $\bar{\Omega}$ grew and these difficulties can be attributed to a number of causes. Following on from work elucidated in Bassom & Hall (1991) it is the case that for small crossflow the most unstable linear mode first has a small wavenumber relative to the implied scaling. As $\hat{\lambda}$ grows then the most unstable mode corresponds to an eigenfunction that moves away from the wall at $y = 0$. At $\bar{\Omega}$ greater than about 2 this movement occurs quickly for small changes in $\hat{\lambda}$ so that for quite moderate values of $\hat{\lambda}$ the eiegnmode is far removed from the boundary. As found both by Bassom & Hall (1991) and Bassom & Otto (1992) the numerical solution of the governing equations becomes non-trivial as the vortex moves out since boundary conditions need to be imposed at the wall. Clearly for modes concentrated away from the wall large changes in $\hat{\beta}$, $\hat{\lambda}$ or $\bar{\Omega}$ can lead to almost imperceptible changes in the values of the eigenfunctions at the wall and thus reliable numerical convergence is rendered very difficult. However, our limited further computations for $\bar{\Omega} > 1.5$ are in agreement with the general behaviour described above.

§5 Conclusions & Discussion

In this work we have detailed the nonlinear spatial evolution of unstable Görtler modes in a three-dimensional boundary layer. In particular, the roles played by vortex wavenumber, frequency, and the crossflow component of the underlying base flow have been described. We feel that of particular importance is our finding that (all other factors being equal) of two modes of wavenumber within the $O(G^{\frac{1}{5}})$ regime the one with the smaller wavelength will be the first to breakdown. This then suggests that in practical situations it may not be the most unstable linear mode which is of ultimate importance.

In many cases the relevant calculation to describe the breakdown of a flow is one of a receptivity type. In this scenario small disturbances within the boundary layer

or on the wall of the cylinder can trigger Görtler vortices and the precise method of this triggering frequently excites modes of a preferred wavenumber. If this occurs in practice then our calculations provide a description of the evolution of the mode. Conversely, if a range of wavenumber modes is excited two eventualities would seem to be possible. First, suppose that the initial disturbance is very small. Then it is to be expected that the perturbation travels a long way downstream before nonlinearity has significant effect, the most unstable linear mode will be dominant before this point and its evolution characteristics will essentially describe that of the whole flow. Second, suppose that the initial perturbation is not so small. Our results summarised by figure 3 have shown that although there is a unique most unstable mode for each crossflow $\hat{\lambda}$ and frequency $\bar{\Omega}$ vortices with wavenumbers in a fairly–large region surrounding that of the most unstable mode have growth rates not very different from the maximum. Therefore, by the time nonlinearity is significant it is not clear that the most unstable mode would be dominant and the breakdown characteristics of the whole flow would involve calculations more involved than those reported here. However we have shown that for given mode amplitude it is the higher–wavenumber modes which appear to breakdown first so that these components of a spectrum of excited modes may well prove to be the important ones.

Denier & Hall (1992) showed that when their calculations for nonlinear modes in two–dimensional boundary layers terminated, this corresponds to the skin friction of the flow vanishing at some point. Once this happens marching schemes as used both here and in Denier & Hall (1992) cannot be continued. We confirm this finding for our three–dimensional cases as well but we also observed that before the skin friction vanishes the velocity profile develop inflection points at positions away from the wall. The appearance of those inflection points suggest that the flow will become susceptible to Rayleigh waves which would give an alternative route to the ultimate breakdown. The analysis of these modes would be of interest.

Finally, we recall that all our calculations have been concerned with considering the evolution of perturbations of a specified wavenumber. Of course in some situations a spectrum of modes may well be present. We have identified situations in which we might expect one mode to dominate the others before nonlinearity sets in but in the other cases calculations would be needed which account for an initial perturbation which contains a number of modes. The development of a code to perform such calculations might well be formidable but it would give the definitive theoretical description of nonlinear Görtler vortex behaviour in three–dimensional boundary layers.

Acknowledgements

The authors wish to acknowledge Drs. Craig Streett, Ralph Smith, Jim Denier and Demetrius Papageorgiou for comments regarding the techniques used herein. The research of SRO was supported by the National Aeronautics and Space Administration under NASA contracts Nos. NAS1-18605 and NAS1-19480 while he was in residence at the Institute for Computer Applications in Science and Engineering (ICASE), NASA Langley Research Center, Hampton, VA 23665, USA. APB would like to thank ICASE for their support and hospitality during a visit whilst part of this work was carried out.

References

Aihara, Y. (1976) Nonlinear analysis of Görtler vortices. *Phys. Fluids* **19** 1655-1660

Bassom, A.P. & Hall, P. (1991) Vortex instabilities in three–dimensional boundary layers: The relationship between Görtler and Crossflow vortices *J. Fluid Mech.* **232** 647–680

Bassom, A. P. & Otto, S.R. (1992) On the stability of nonlinear viscous vortices in three–dimensional boundary layers. *ICASE Report No. 92-15, submitted to J. Fluid Mech.*

Cooley, J. W. & Tukey, J. W. (1965) An Algorithm for the Machine Calculation of Complex Fourier Series *Mathematics of Computation* **19** 297–301

Denier, J.P. & Hall, P. (1991) On the nonlinear development of the most unstable Görtler vortex mode *ICASE Report No. 91-86, submitted to J. Fluid Mech.*

Denier, J.P., Hall, P. & Seddougui, S. (1991) On the receptivity problem for Görtler vortices: vortex motion induced by wall roughness *Phil. Trans. Roy. Soc. Lond. A* **335** 51–85

Görtler, H. (1940) Uber eine dreidimensionale instabilität laminare Grenzschubten an Konkaven Wänden *NACA TM 1357*

Hall, P. (1982a) Taylor–Görtler vortices in fully developed or boundary layer flows *J. Fluid Mech.* **124** 475–494

Hall, P. (1982b) On the nonlinear evolution of Görtler vortices in non–parallel boundary layers *J. Inst. Maths Applics* **29** 173–196

Hall, P. (1985) The Görtler vortex instability mechanism in three–dimensional boundary layers *Proc. Roy. Soc. Lond. A* **399** 135–152

Hall, P. (1988) The nonlinear development of Görtler vortices in growing boundary layers *J. Fluid Mech.* **193** 247–266

Hall, P. (1990) Görtler vortices in growing boundary layers: the leading edge receptivity problem, linear growth and the nonlinear breakdown stage *Mathematika* **37** 151–189

Hämmerlin, G. (1956) Zur Theorie der dreidimensionalen Instabilitat laminar Grenschichten *Z. Angew. Math. Phys.* **1** 156–167

Macaraeg, M. G., Streett, C. L. & Hussaini, M. Y. (1988) A Spectral Collocation Solution to the Compressible Stability Eigenvalue Problem. *NASA technical Paper* **2858**

Smith, A.M.O. (1955) On the growth of Taylor–Görtler vortices along highly concave walls *Q. Appl. Maths* **13** 233–262

Stuart, J.T. (1960) On the nonlinear mechanics of wave disturbances in stable and unstable parallel flows, Part 1. The basic behaviour in plane Poiseuille flow *J. Fluid Mech.* **9** 353–370

Timoshin, S. N. (1990) Asymptotic Analysis of a Spatially Unstable Görtler Vortex Spectrum. *Fluid Dynamics* **25** 25–33

Watson, J. (1960) On the nonlinear mechanics of wave disturbances in stable and unstable parallel flows, Part 2. The development of a solution for plane Poiseuille and plane Couette flow *J. Fluid Mech.* **9** 371–389

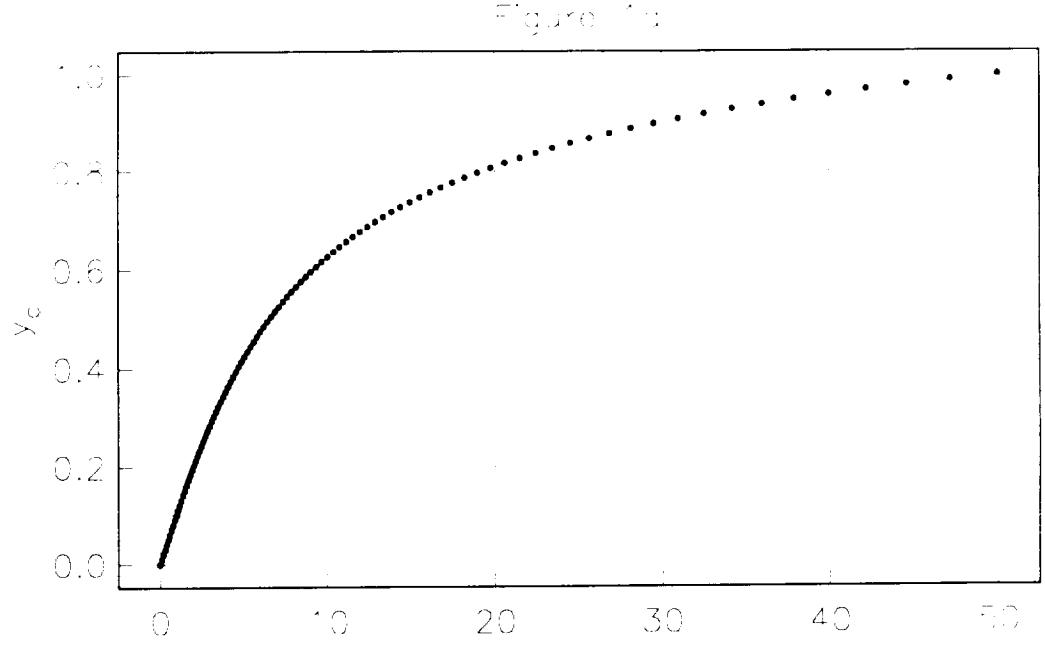

Figure 1a

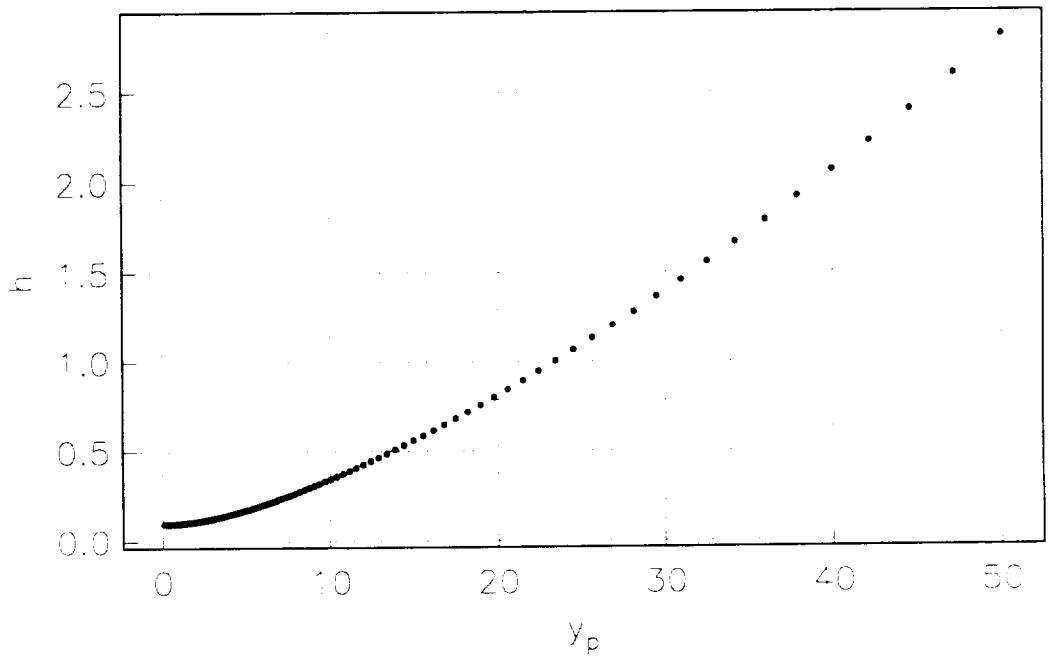

Figure 1b

Figure 1: Distribution of grid points and corresponding spacing for the calculations performed here. The computational coordinate y_c satisfies $0 \leq y_c \leq 1$ and is related to the physical coordinate y_p by $y_p = 50y_c/(2 - y_c^2)^{2.4}$.

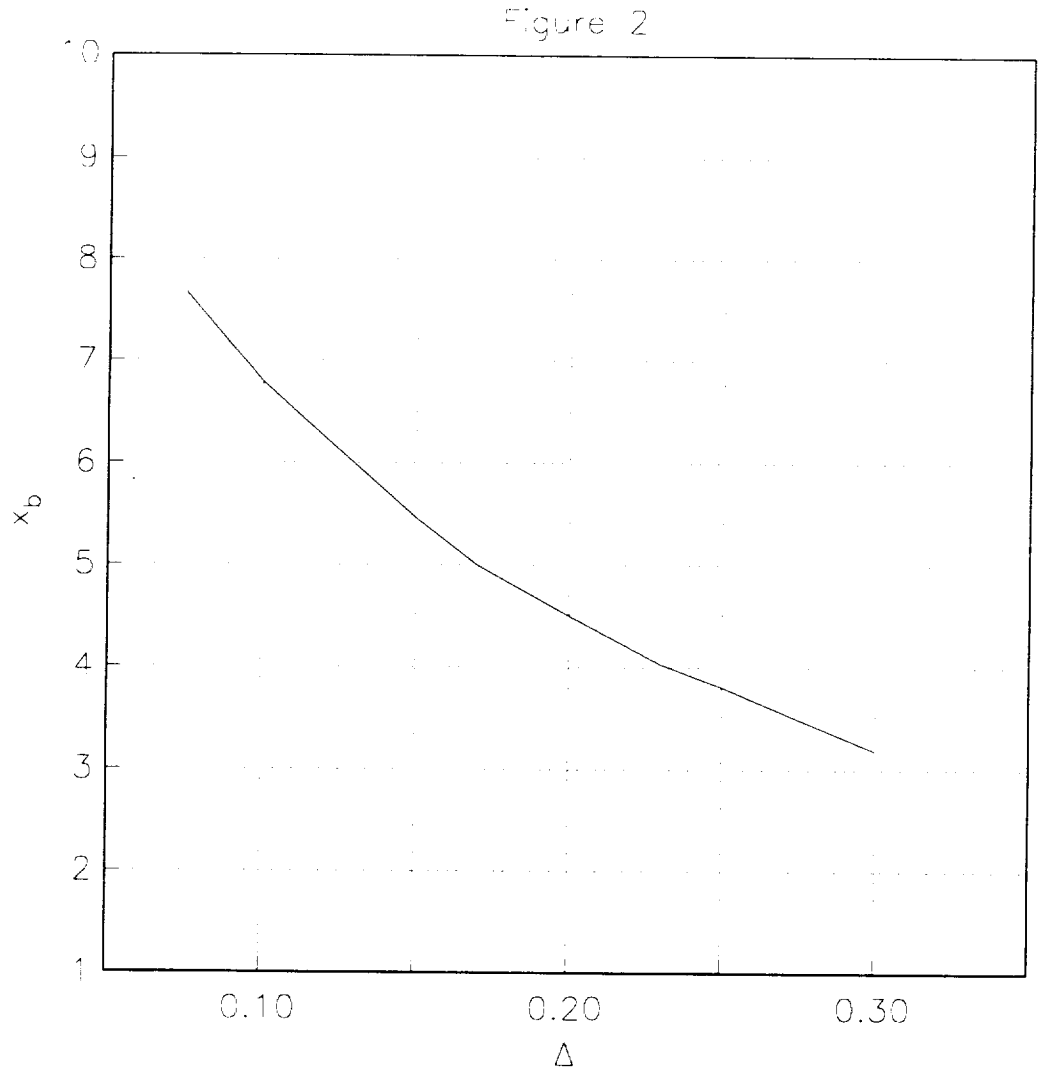

Figure 2: Location of breakdown point x_b as a function of initial vortex amplitude Δ for the most unstable mode with $\hat{\lambda} = 0$, $\bar{\Omega} = 0$.

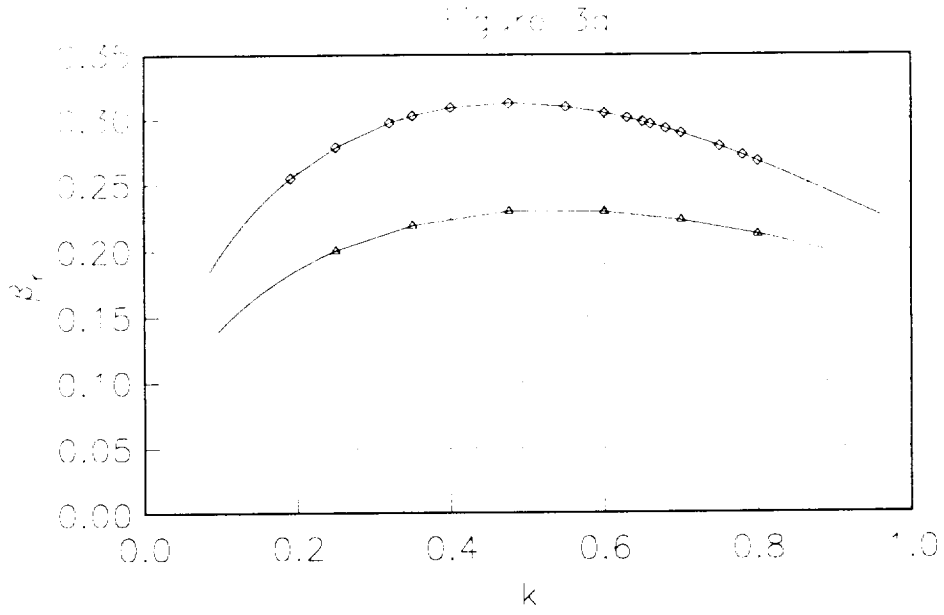

Figure 3b

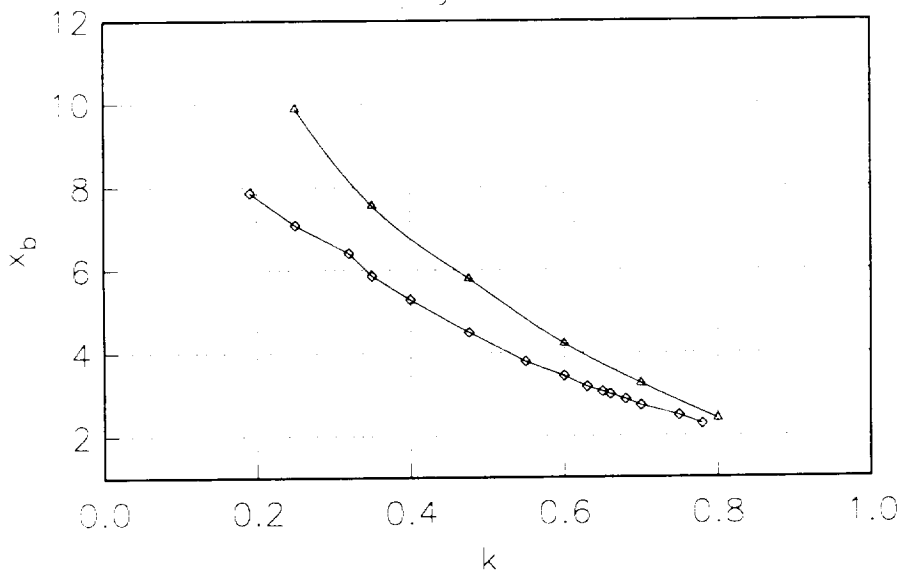

Figure 3:
a) Linear vortex growth rates β_r as a function of wavenumber k for the two most dangerous modes in a two-dimensional boundary layer.
b) Breakdown point x_b as a function of wavenumber k for the modes in figure 3a with assumed initial amplitude $\Delta = 0.2$. The symbols denote corresponding points on the curves of a) and b).

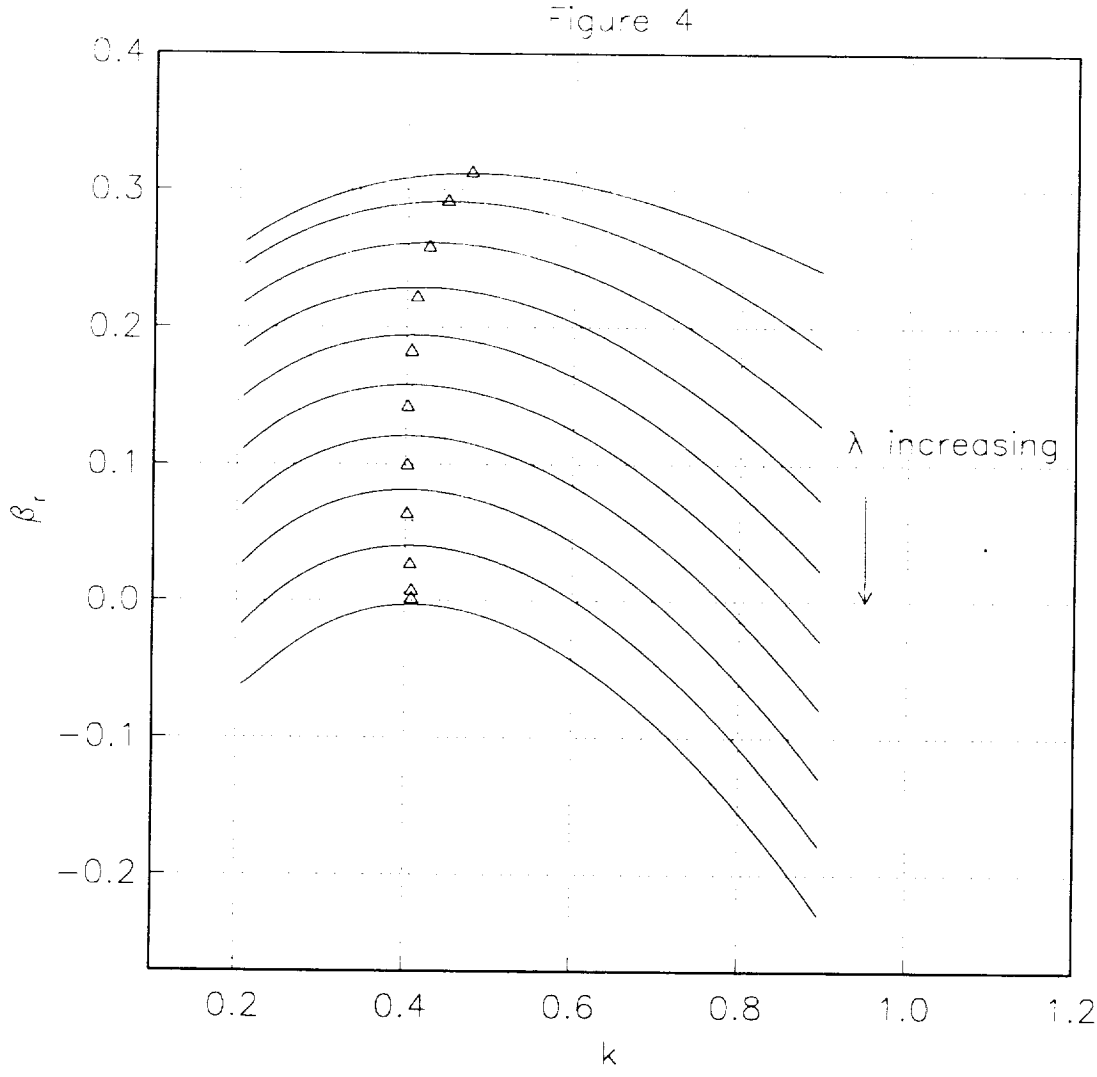

Figure 4: Growth rate of β_r of the most dangerous stationary vortex modes within a boundary layer with increasing crossflow $\hat{\lambda}$. The curves correspond to $\hat{\lambda}$ varying between 0.005 and 0.410 in 9 equal steps. The indicated points show the locus of the wavenumber of the most unstable mode as the crossflow varies.

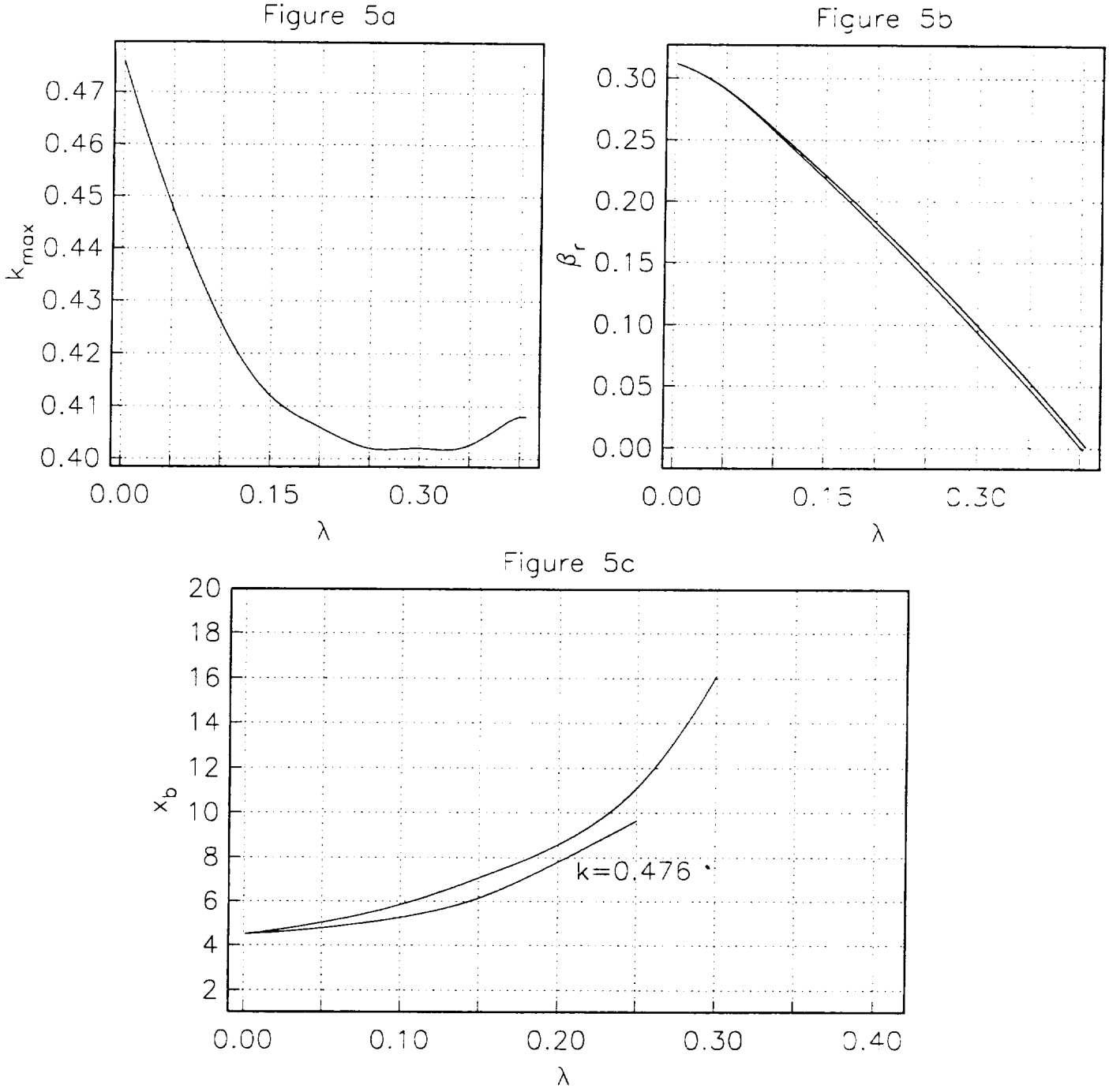

Figure 5:
a) Wavenumber of the most unstable stationary mode and b) its corresponding growth rate as a function of crossflow $\hat{\lambda}$.
c) Breakdown point x_b as a function of crossflow $\hat{\lambda}$ for *i*) the most unstable mode and *ii*) the mode with $k = 0.476$ for initial amplitude $\Delta = 0.2$.

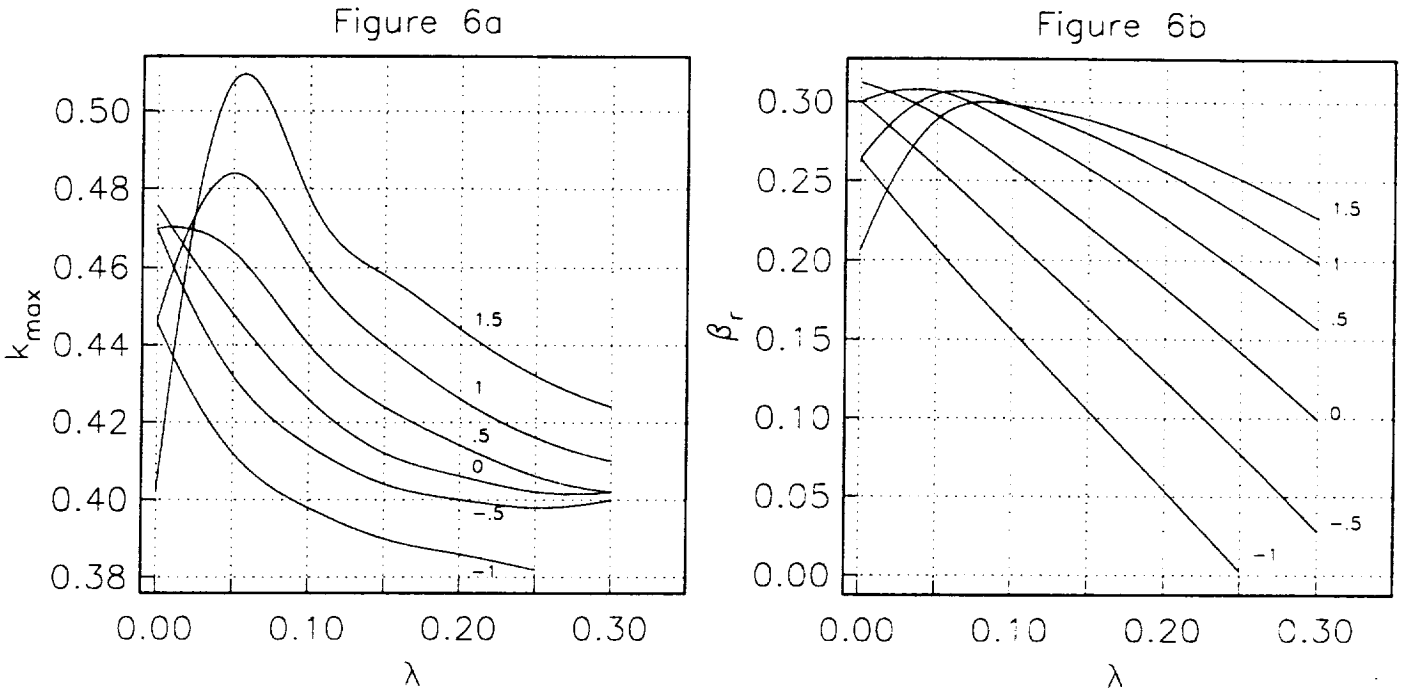

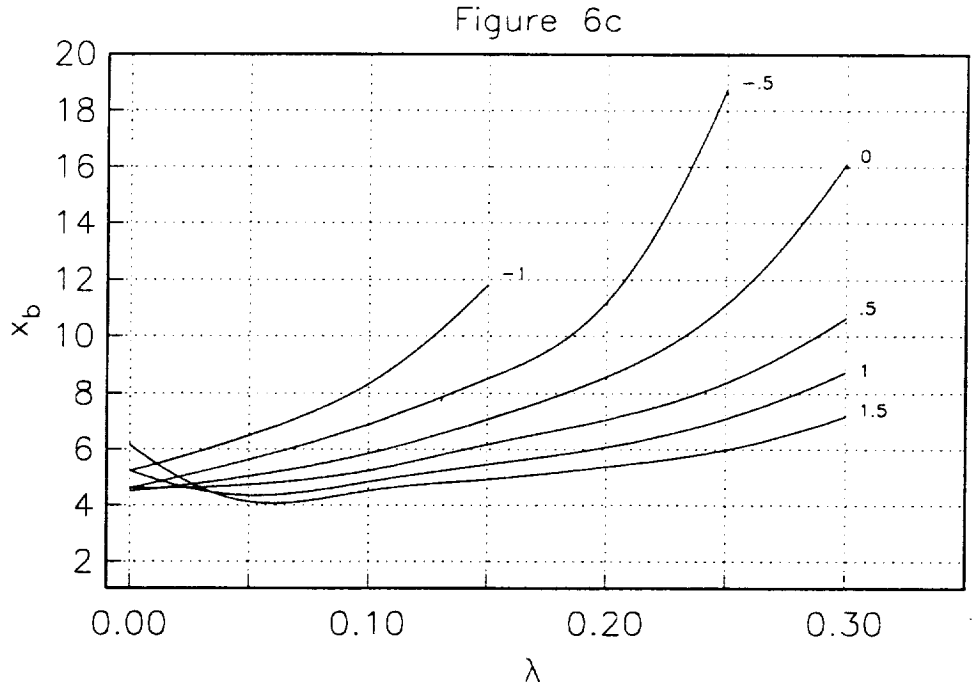

Figure 6:
a) Wavenumber of the most unstable nonstationary modes and b) corresponding growth rates β_r as functions of $\hat{\lambda}$. Here we have considered $\bar{\Omega} = -1, 0.5, 0, 0.5, 1, 1.5$.
c) Breakdown point x_b as a function of crossflow $\hat{\lambda}$ for the modes with frequencies $\bar{\Omega}$ and wavenumbers k as given in figure 6a) and initial amplitude $\Delta = 0.2$.